

## FULL PAPER

# Four-, five- and six-coordinated transition metal complexes based on naphthalimide Schiff base ligands: Synthesis, crystal structure and properties

Yuling Xu | Han Zhang | Kesheng Shen | Shanshan Mao | Xinkui Shi | Huilu Wu 

School of Chemical and Biological Engineering, Lanzhou Jiaotong University, Lanzhou, Gansu 730070, People's Republic of China

**Correspondence**

Huilu Wu, School of Chemical and Biological Engineering, Lanzhou Jiaotong University, Lanzhou, Gansu 730070, People's Republic of China.  
Email: wuhuilu@163.com

**Funding information**

Lanzhou Jiaotong University; Natural Science Foundation of Gansu Province, Grant/Award Number: 1212RJZA037; National Natural Science Foundation of China, Grant/Award Number: 21367017

Two bidentate Schiff base ligands ( $HL^1 = N$ -*n*-butyl-4-[(*E*)-2-(((2-aminoethyl)imino)methyl)phenol]-1,8-naphthalimide; and  $HL^2 = N$ -*n*-butyl-4-[(*E*)-2-(((2-aminoethyl)imino)methyl)-6-methoxyphenol]-1,8-naphthalimide) with their metal complexes  $[Cu(L^1)_2]$  (**1**),  $[Zn(L^1)_2(Py)]_2 \cdot H_2O$  (**2**) and  $[Ni(L^2)_2(DMF)_2]$  (**3**) have been synthesized and characterized. Single-crystal X-ray structure analysis reveals that complex **1** has a four-coordinated square geometry, while complex **2** is a five-coordinated square pyramidal structure and complex **3** is a distorted six-coordinated octahedral structure. Cyclic voltammograms of **1** indicate an irreversible  $Cu^{2+}/Cu^+$  couple. *In vitro* antioxidant activity assay demonstrates that the ligands and the two complexes **1** and **3** display high scavenging activity against hydroxyl ( $HO^\bullet$ ) and superoxide ( $O_2^{\bullet-}$ ) radicals. Moreover, the fluorescence properties of the ligands and complexes **1–3** were studied in the solid state. Metal-mediated enhancement is observed in **2**, whereas metal-mediated fluorescence quenching occurs with **1** and **3**.

**KEYWORDS**

antioxidant, crystal structure, fluorescence, naphthalimide Schiff base, transition metal complexes

## 1 | INTRODUCTION

In recent years, transition metal complexes based on Schiff base ligands have been extensively studied for their novel structure and potential application value in many fields.<sup>[1]</sup> In particular, a considerable number of transition metal complexes of Schiff base ligands formed by the condensation of salicylaldehyde with primary amines have become a hot topic in current research.<sup>[2]</sup> These Schiff base ligands contain bidentate N,O-<sup>[3]</sup> and tridentate N,O,O-donor groups,<sup>[4]</sup> and so on, which can be designed to form mono-, di-, trimeric, one-, two-, three-dimensional complexes together with other coordinating moieties such as thiocyanate and carboxylic groups acting as either bridging or terminal ligands.<sup>[5]</sup> Strong anticancer activities were found for Schiff base complexes derived from 4-hydroxysalicylaldehyde and amines.<sup>[6]</sup> Prevalent related work reported that the activity of drugs increased when administered as metal complexes rather than as organic

compounds.<sup>[7,8]</sup> It has been suggested that the azomethine linkages are responsible for the biological activities of Schiff bases, such as antitumor, antimicrobial, antifungal and herbicidal activities.<sup>[9]</sup>

1,8-Naphthalimide derivatives have been widely used in many fields involving optical, electrical and biological aspects, such as coloring and whitening of polymers,<sup>[10]</sup> potential photobiochemical units,<sup>[11]</sup> bioluminescent labeling,<sup>[12]</sup> light-emitting diodes,<sup>[13]</sup> fluorescent detectors and switches,<sup>[14]</sup> electroluminescent materials<sup>[15]</sup> and liquid crystal displays.<sup>[16]</sup> A large variety of auxiliary color-changing groups in 1,8-naphthalimide derivatives can be easily grafted to fine tune the absorption and emission wavelengths. In our previous work, we have investigated the coordinating ability of some kinds of linear ester Schiff base ligands and complexes.<sup>[17]</sup> Little is known on the use of 1,8-naphthalimide derivatives to form Schiff base complexes with salicylaldehyde and *o*-vanillin. Hence, in this

article, we report the synthesis, structure, fluorescence and electrochemical properties, and antioxidant activity of three transition metal complexes containing naphthalimide Schiff base ligands.

## 2 | EXPERIMENTAL

### 2.1 | General Methods

All chemicals and solvents were of reagent grade and were used without further purification. C, H and N elemental analyses were performed using a Carlo Erba 1106 elemental analyzer. The thermal analyses of the complexes were carried out under nitrogen atmosphere with a heating rate of  $10\text{ }^{\circ}\text{C min}^{-1}$  with a Mettler Toledo TGA1. Infrared (IR) spectra were recorded in the range  $400\text{--}4000\text{ cm}^{-1}$  with a Nicolet FT-VERTEX 70 spectrometer using KBr pellets. Electronic spectra were obtained with a Lab-Tech UV Bluestar spectrophotometer. Absorbance was measured with a Spectrumlab 722sp spectrophotometer at room temperature.  $^1\text{H NMR}$  spectra were recorded with a Varian VR 300 MHz spectrometer using tetramethylsilane as an internal standard. Fluorescence measurements were performed with a 970-CRT spectrofluorophotometer. Electrochemical measurements were performed with an LK2005A electrochemical analyzer under nitrogen at 283 K. A glassy carbon working electrode, a platinum wire auxiliary electrode and an Ag/AgCl reference electrode ( $[\text{Cl}^-] = 1.0\text{ mol dm}^{-3}$ ) were used in the three-electrode measurements. The electroactive component was at a concentration of  $1.0 \times 10^{-3}\text{ mol}\cdot\text{dm}^{-3}$  with tetrabutylammonium perchlorate ( $0.1\text{ mol dm}^{-3}$ ) used as the supporting electrolyte in dimethylformamide (DMF). The antioxidant activities with superoxide anion radical ( $\text{O}_2^{\bullet-}$ ) and hydroxyl radical ( $\text{HO}^{\bullet}$ ) were investigated using a water bath with a 722sp spectrophotometer. The synthetic route to the free ligands  $\text{HL}^1$  and  $\text{HL}^2$  is shown in Scheme 1.

## 2.2 | Synthesis of Ligands and Transition Metal Complexes

### 2.2.1 | 4-Bromo-*N-n*-butyl-1,8-naphthalimide

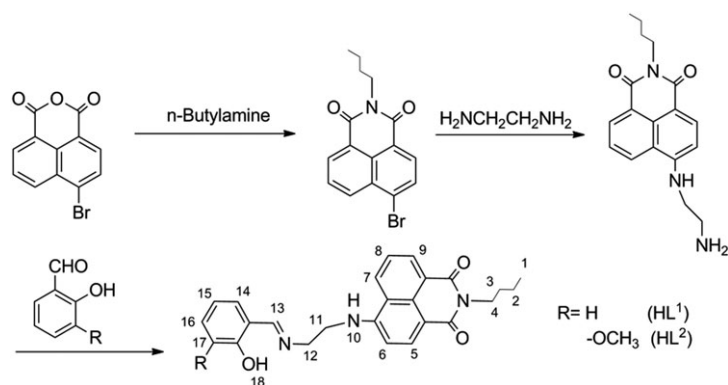
A suspension of 4-bromo-1,8-naphthalic anhydride (15 g, 0.054 mol) and *n*-butylamine (7.90 g, 0.108 mol) in 300 ml of ethanol was refluxed with stirring for 3 h. After the reaction was complete, the reaction mixture was cooled to room temperature and the solid phase was filtered off, washed with ethanol and dried to afford 17 g of pure 4-bromo-*N-n*-butyl-1,8-naphthalimide as light yellow solid. Yield 94.5%; m.p.  $107\text{--}109\text{ }^{\circ}\text{C}$  (lit.<sup>[18]</sup>  $109\text{--}110\text{ }^{\circ}\text{C}$ ).

### 2.2.2 | 4-(2-Aminoethyl)amino-*N-n*-butyl-1,8-naphthalimide

An amount of 1.0 g (3.01 mmol) of 4-bromo-*N-n*-butyl-1,8-naphthalimide was added to 12.2 g (201.67 mmol) of ethylenediamine in a 100 ml flask. The reaction mixture was stirred and heated to reflux for 3 h. After completion of the reaction, the final solution was cooled to room temperature and then treated with 10 ml of distilled water. The resulting precipitate was collected by filtration, washed with distilled water and dried in air. Recrystallization of 0.50 g of this product from toluene afforded 0.26 g (52%) of 4-(2-aminoethyl)amino-*N-n*-butyl-1,8-naphthalimide as a yellow-orange solid; m.p.  $129\text{--}132\text{ }^{\circ}\text{C}$  (lit.<sup>[18]</sup>  $128\text{--}131\text{ }^{\circ}\text{C}$ ).

### 2.2.3 | *N-n*-Butyl-4-[(*E*)-2-(((2-aminoethyl)imino)methyl)phenol]-1,8-naphthalimide ( $\text{HL}^1$ )

A solution of excess salicylic aldehyde (0.39 g, 3.22 mmol) in 10 ml of ethanol was added dropwise to a solution of 0.5 g (1.61 mmol) of the intermediate 4-(2-aminoethyl)amino-*N-n*-butyl-1,8-naphthalimide in 30 ml of absolute ethanol in a period of 10 min. The reaction mixture was refluxed



**SCHEME 1** Synthetic route to ligands  $\text{HL}^1$  and  $\text{HL}^2$

for 4 h and then cooled to room temperature. The resulting precipitate was filtered and washed with ethanol.

Yield 71.6%; m.p. 136–138 °C. Anal. Calcd for  $C_{25}H_{25}N_3O_3$  (%): C, 72.27; H, 6.06; N, 10.11. Found (%): C, 72.20; H, 6.11; N, 10.08. IR (KBr;  $\nu$ ,  $cm^{-1}$ ): 1634  $\nu(C=N)$ , 1617  $\nu(C=C)$ , 1277  $\nu(C-O)$ ; O in Ph), 1245  $\nu(C-N)$ . UV–visible (DMF, nm): 282, 325, 436. MS: ( $[C_{25}H_{25}N_3O_3]^+$ )  $m/z$  = 416.2141.  $^1H$  NMR (400 MHz, DMSO- $d_6$ ,  $\delta$ , ppm): 13.36 (s, 1H), 8.67 (d,  $J$  = 8 Hz, 1H, H9), 8.56 (s, 1H, H13), 8.43 (d,  $J$  = 8 Hz, 1H, H7), 8.26 (d,  $J$  = 8 Hz, 1H, H5), 7.91 (s, 1H, H10), 7.68 (t, 16 Hz, 1H, H8), 7.38 (d,  $J$  = 8 Hz, 1H, H14), 7.31 (t,  $J$  = 16 Hz, 1H, H16), 6.93 (d,  $J$  = 12 Hz, 1H, H6), 6.87 (d,  $J$  = 8 Hz, 1H, H15), 6.84 (s, 1H, H17), 3.99–4.03 (m, 2H, N–CH<sub>2</sub>–CH<sub>2</sub>–N), 3.94 (d, 2H, –CH<sub>2</sub>–N–), 3.76 (d, 2H, H<sub>2</sub>O), 1.55–1.62 (m, 2H, C3), 1.31–1.38 (m, 2H, C2), 0.92 (t, 3H, –CH<sub>3</sub>).  $^{13}C$  NMR (400 MHz, DMSO- $d_6$ ,  $\delta$ , ppm): 167.64, 164.29, 163.48, 161.25, 150.97, 134.61, 132.96, 132.28, 131.16, 129.93, 128.95, 124.84, 122.49, 120.77, 119.32, 119.11, 117.11, 108.68, 104.64, 57.36, 44.11, 39.99, 30.49, 20.53, 14.40.

### 2.2.4 | *N-n*-Butyl-4-[(*E*)-2-(((2-aminoethyl)imino)methyl)-6-methoxyphenol]-1,8-naphthalimide (HL<sup>2</sup>)

A solution of excess *o*-vanillin 0.49 g (3.22 mmol) in 10 ml of ethanol was added dropwise to a solution of 0.5 g (1.61 mmol) of the intermediate 4-(2-aminoethyl)amino-*N-n*-butyl-1,8-naphthalimide in 30 ml of absolute ethanol in a period of 10 min. The reaction mixture was refluxed for 4 h and then cooled to room temperature. The resulting precipitate was filtered and washed with ethanol.

Yield 61.1%; m.p. 189–191 °C. Anal. Calcd for  $C_{26}H_{27}N_3O_4$  (%): C, 70.09; H, 6.11; N, 9.43. Found (%): C, 70.14; H, 6.08; N, 9.40. IR (KBr;  $\nu$ ,  $cm^{-1}$ ): 1645  $\nu(C=N)$ , 1614  $\nu(C=C)$ , 1252  $\nu(C-O)$ ; O in Ph), 1227  $\nu(C-N)$ . UV–visible (DMF, nm): 327, 437. MS: ( $[C_{26}H_{27}N_3O_4]^+$ )  $m/z$  = 446.2276.  $^1H$  NMR (400 MHz, DMSO- $d_6$ ,  $\delta$ , ppm): 13.54 (s, 1H), 8.65 (d,  $J$  = 8 Hz, 1H, H9), 8.53 (s, 1H, H13), 8.41 (d,  $J$  = 8 Hz, 1H, H7), 8.24 (d,  $J$  = 8 Hz, 1H, H5), 7.89 (s, 1H, H10), 7.66 (t, 16 Hz, 1H, H8), 7.00 (d,  $J$  = 8 Hz, 1H, H6), 6.95 (d,  $J$  = 8 Hz, 1H, H14), 6.90 (d,  $J$  = 8 Hz, 1H, H16), 6.76 (t,  $J$  = 16 Hz, 1H, H15), 4.00 (t, 2H, –CH<sub>2</sub>–N–), 3.76 (s, 3H, CH<sub>3</sub>–O–), 1.58 (m, 2H, C3), 1.30–1.36 (m, 2H, C2), 0.92 (t, 3H, –CH<sub>3</sub>).  $^{13}C$  NMR (400 MHz, DMSO- $d_6$ ,  $\delta$ , ppm): 167.03, 163.55, 162.74, 151.93, 150.20, 148.08, 133.82, 130.37, 129.16, 128.17, 124.03, 123.13, 121.74, 120.01, 118.25, 117.46, 114.65, 108.01, 103.83, 56.09, 55.65, 43.45, 39.49, 29.79, 19.85, 13.69.

### 2.2.5 | Synthesis of metal complexes

A general method was used for the preparation of the complexes using reaction of metal salts and the corresponding Schiff bases in a molar ratio (M:L) of 1:2. Complexes  $[Cu(L^1)_2]$  (**1**),  $[Zn(L^1)_2(Py)]_2 \cdot H_2O$  (**2**) and  $[Ni(L^2)_2(DMF)_2]$  (**3**) were obtained using a similar procedure. To a stirred solution of ligand HL<sup>1</sup> (0.20 mmol, 83.1 mg) or HL<sup>2</sup> (0.20 mmol, 89.1 mg) in methanol (5 ml) and acetone (5 ml) was added metal salt (0.1 mmol): Cu(CH<sub>3</sub>COO)<sub>2</sub>·H<sub>2</sub>O (20.0 mg), Zn(NO<sub>3</sub>)<sub>2</sub>·6H<sub>2</sub>O (29.1 mg) or Ni(CH<sub>3</sub>COO)<sub>2</sub>·4H<sub>2</sub>O (24.9 mg) in methanol (5 ml). The sediment generated rapidly. The precipitate was filtered off, washed with methanol and dried *in vacuo*. The dried precipitates of complexes **1** and **3** were dissolved in DMF, and complex **2** was dissolved in DMF and pyridine (3:1 *v/v*), to form a yellow solution that was allowed to evaporate at room temperature. Crystals suitable for X-ray diffraction studies were obtained after several days.

Complex **1**. Yield 53%. Anal. Calcd for  $C_{50}H_{48}CuN_6O_6$  (%): C, 67.29; H, 5.42; N, 9.42. Found (%): C, 67.33; H, 5.44; N, 9.46. IR (KBr;  $\nu$ ,  $cm^{-1}$ ): 1151  $\nu(C-N-C)$ , 1352  $\nu(C-O)$ , 1618  $\nu(C=N)$ , 1685  $\nu(C=O)$ . UV–visible (DMF,  $\lambda_{max}$ , nm): 271, 343, 435.

Complex **2**. Yield 51%. Anal. Calcd for  $C_{110}H_{108}N_{14}O_{13}Zn_2$  (%): C, 67.24; H, 5.54; N, 9.98. Found (%): C, 67.25; H, 5.52; N, 9.95. IR (KBr;  $\nu$ ,  $cm^{-1}$ ): 1130  $\nu(C-N-C)$ , 1300  $\nu(C-O)$ , 1620  $\nu(C=N)$ , 1686  $\nu(C=O)$ . UV–visible (DMF,  $\lambda_{max}$ , nm): 278, 341, 436.

Complex **3**. Yield 54%. Anal. Calcd for  $C_{58}H_{66}N_8NiO_{10}$  (%): C, 63.68; H, 6.08; N, 10.24. Found (%): C, 63.65; H, 6.11; N, 10.20. IR (KBr;  $\nu$ ,  $cm^{-1}$ ): 1171  $\nu(C-N-C)$ , 1358  $\nu(C-O)$ , 1643  $\nu(C=N)$ , 1683  $\nu(C=O)$ . UV–visible (DMF,  $\lambda_{max}$ , nm): 276, 329, 435.

### 2.3 | X-ray Crystallography

Suitable single crystals of complexes **1–3** were mounted on a glass fiber, and the intensity data were collected using a Bruker APEX II area detector with graphite-monochromated Mo K $\alpha$  radiation ( $\lambda$  = 0.71073 Å) at 296(2) K. Data reduction and cell refinement were performed using the SMART and SAINT programs.<sup>[19]</sup> The absorption corrections are carried out by the empirical method. The structure was solved by direct methods and refined by full-matrix least squares against  $F^2$  of data using SHELXTL software.<sup>[20]</sup> All H atoms were found in different electron maps and were subsequently refined in a riding model approximation with C–H distances ranging from 0.95 to 0.99 Å. Information concerning the crystallographic data collection and structural refinements is summarized in Table 1. The relevant bond lengths and angles are listed in Table 2.

**TABLE 1** Crystal and structure refinement data for complexes 1–3

	1	2	3
Empirical formula	C <sub>50</sub> H <sub>48</sub> CuN <sub>6</sub> O <sub>6</sub>	C <sub>110</sub> H <sub>108</sub> N <sub>14</sub> O <sub>13</sub> Zn <sub>2</sub>	C <sub>58</sub> H <sub>66</sub> N <sub>8</sub> NiO <sub>10</sub>
Molecular weight (g mol <sup>-1</sup> )	892.48	1964.84	1093.90
Crystal system	Monoclinic	Triclinic	Monoclinic
Space group	C2/c	P-1	P2(1)/c
Unit cell dimensions			
<i>a</i> (Å)	33.685(7)	16.519(3)	14.286(4)
<i>b</i> (Å)	12.629(3)	17.488(3)	27.128(8)
<i>c</i> (Å)	23.909(5)	17.795(3)	9.637(3)
$\alpha$ (°)	90	81.057(4)	90
$\beta$ (°)	121.271(3)	86.043(4)	132.344(5)
$\gamma$ (°)	90	80.657(3)	90
Volume (Å <sup>3</sup> )	8693(3)	5005.8(16)	2760.4(14)
Z	8	2	2
<i>D</i> (calculated) (g cm <sup>-3</sup> )	1.364	1.304	1.316
Absorption coefficient (mm <sup>-1</sup> )	0.561	0.549	0.417
<i>F</i> (000)	3736	2060	1156
$\theta$ range for data collection (°)	1.41 to 25.11	1.54 to 25.09	1.50 to 25.50
Reflections collected	21 527	25 513	11 014
Independent reflections	7698 [ <i>R</i> (int) = 0.0589]	17 533 [ <i>R</i> (int) = 0.0544]	4090 [ <i>R</i> (int) = 0.0435]
Goodness-of-fit on <i>F</i> <sup>2</sup>	1.017	0.904	0.900
Final <i>R</i> <sub>1</sub> and <i>wR</i> <sub>2</sub> [ <i>I</i> > 2 $\sigma$ ( <i>I</i> )]	<i>R</i> <sub>1</sub> = 0.0618, <i>wR</i> <sub>2</sub> = 0.1704	<i>R</i> <sub>1</sub> = 0.0842, <i>wR</i> <sub>2</sub> = 0.2096	<i>R</i> <sub>1</sub> = 0.0475, <i>wR</i> <sub>2</sub> = 0.1148
<i>R</i> indices (all data)	<i>R</i> <sub>1</sub> = 0.1097, <i>wR</i> <sub>2</sub> = 0.2067	<i>R</i> <sub>1</sub> = 0.1887, <i>wR</i> <sub>2</sub> = 0.2487	<i>R</i> <sub>1</sub> = 0.0790, <i>wR</i> <sub>2</sub> = 0.1266

## 2.4 | Antioxidant Activities

### 2.4.1 | Hydroxyl radical scavenging activity

Hydroxyl radicals in aqueous media were generated through the Fenton-type reaction.<sup>[21,22]</sup> Aliquots of the reaction mixture (3 ml) contained 1 ml of 0.1 mM aqueous safranin, 1 ml of 1.0 mM aqueous EDTA–Fe(II), 1 ml of 3% aqueous H<sub>2</sub>O<sub>2</sub> and a series of quantitative microadditions of solutions of the test compound. The sample without the test compounds was used as the control. The reaction mixtures were incubated at 37 °C for 30 min in a water bath. Absorbance at 520 nm was measured and the solvent effect was corrected throughout. The scavenging effect for HO• was calculated from the following expression<sup>[23]</sup>:

$$\text{Scavenging effect (\%)} = \frac{A_{\text{sample}} - A_r}{A_0 - A_r} \times 100$$

where *A*<sub>sample</sub> is the absorbance of the sample in the presence of the test compound, *A*<sub>r</sub> is the absorbance of the blank in the absence of the test compound and *A*<sub>0</sub> is the absorbance in the absence of the test compound and EDTA–Fe(II).

### 2.4.2 | Superoxide radical scavenging activity

A non-enzymatic system containing 1 ml of 9.9 × 10<sup>-6</sup> M VitB<sub>2</sub>, 1 ml of 1.38 × 10<sup>-4</sup> M NBT and 1 ml of 0.03 M

MET was used to produce superoxide anion (O<sub>2</sub><sup>-•</sup>). The scavenging rate of O<sub>2</sub><sup>-•</sup> under the influence of 0.1–1.0 μM of the test compound was determined by monitoring the reduction in the rate of transformation of NBT to monoformazan dye. The details of the methods are given elsewhere.<sup>[24]</sup> The reactions were monitored at 560 nm with a UV–visible spectrophotometer, and the rate of change of absorption was determined. The percentage inhibition of NBT reduction was calculated using the following equation<sup>[25]</sup>:

$$\text{Inhibition of NBT reduction (\%)} = \frac{1 - k'}{k} \times 100$$

where *k'* and *k* are the slopes of the straight lines of absorbance as a function of time in the presence and absence of superoxide dismutase (SOD) mimic compound, respectively.

## 3 | RESULTS AND DISCUSSION

Scheme 1 summarizes the multi-step procedure leading to the ligands HL<sup>1</sup> and HL<sup>2</sup>. In the present investigations, three complexes were synthesized and characterized using various physical and chemical techniques. The complexes are soluble in polar aprotic solvents such as DMF, DMSO and MeCN, slightly soluble in ethanol, methanol, ethyl acetate, acetone and chloroform, and partially soluble in water and Et<sub>2</sub>O.

**TABLE 2** Selected bond distances (Å) and angles (°) for complexes 1–3

Complex 1			
Cu(1)–O(3)	1.884(3)	Cu(1)–O(6)	1.884(3)
Cu(1)–N(3)	2.000(4)	Cu(1)–N(6)	1.992(4)
O(3)–Cu(1)–O(6)	169.63(17)	O(3)–Cu(1)–N(6)	87.81(15)
O(6)–Cu(1)–N(6)	92.42(15)	O(3)–Cu(1)–N(3)	92.13(14)
O(6)–Cu(1)–N(3)	89.61(15)	N(6)–Cu(1)–N(3)	169.05(14)
Complex 2			
Zn(1)–O(1)	1.973(5)	Zn(1)–O(2)	1.982(4)
Zn(1)–N(6A)	2.100(5)	Zn(1)–N(7)	2.109(5)
Zn(1)–N(0AA)	2.127(5)	Zn(2)–O(3)	1.973(5)
Zn(2)–O(4)	1.989(5)	Zn(2)–N(75)	2.056(12)
Zn(2)–N(6)	2.113(6)	Zn(2)–N(3)	2.125(6)
Zn(2)–N(75A)	2.130(17)		
O(1)–Zn(1)–O(2)	162.57(18)	O(1)–Zn(1)–N(6A)	98.5(2)
O(2)–Zn(1)–N(6A)	98.9(2)	O(1)–Zn(1)–N(7)	88.1(2)
O(2)–Zn(1)–N(7)	88.8(2)	N(6A)–Zn(1)–N(7)	99.54(19)
O(1)–Zn(1)–N(0AA)	87.2(2)	O(2)–Zn(1)–N(0AA)	88.03(19)
N(6A)–Zn(1)–N(0AA)	106.9(2)	N(7)–Zn(1)–N(0AA)	153.52(19)
O(3)–Zn(2)–O(4)	161.10(18)	O(3)–Zn(2)–N(75)	103.3(5)
O(4)–Zn(2)–N(75)	95.6(5)	O(3)–Zn(2)–N(6)	87.0(2)
O(4)–Zn(2)–N(6)	89.7(2)	N(75)–Zn(2)–N(6)	100.3(5)
O(3)–Zn(2)–N(3)	88.6(2)	O(4)–Zn(2)–N(3)	85.8(2)
N(75)–Zn(2)–N(3)	107.2(5)	N(6)–Zn(2)–N(3)	152.4(2)
O(3)–Zn(2)–N(75A)	99.8(6)	O(4)–Zn(2)–N(75A)	99.1(6)
N(75)–Zn(2)–N(75A)	3.5(7)	N(6)–Zn(2)–N(75A)	99.9(5)
N(3)–Zn(2)–N(75A)	107.8(5)		
Complex 3			
Ni(1)–O(1)	2.013(2)	Ni(1)–N(1)	2.068(3)
Ni(1)–O(5)	2.143(2)	Ni(1)–O(1)A#1	2.013(2)
Ni(1)–N(1)A#1	2.068(3)	Ni(1)–O(5)A#1	2.143(2)
O(1)–Ni(1)–N(1)	89.26(9)	O(1)–Ni(1)–O(5)	89.48(9)
N(1)–Ni(1)–O(5)	93.58(10)	O(1)A#1–Ni(1)–O(1)	180.0
N(1)A#1–Ni(1)–N(1)	180.00(10)	N(1)A#1–Ni(1)–O(5)	86.42(10)
O(1)–Ni(1)–N(1)A#1	90.74(9)	O(1)A#1–Ni(1)–O(5)	90.52(9)

Elemental analysis shows that their compositions are  $[\text{Cu}(\text{L}^1)_2]$ ,  $[\text{Zn}(\text{L}^1)_2(\text{Py})]_2 \cdot \text{H}_2\text{O}$  and  $[\text{Ni}(\text{L}^2)_2(\text{DMF})_2]$ , which are confirmed by crystal structure analysis.

### 3.1 | IR and UV Spectra

The IR spectral data for the free ligands and the three metal complexes with their relative assignments were used to characterize their structures. The IR spectrum of  $\text{HL}^2$  is closely related to that of the free ligand  $\text{HL}^1$ . The spectrum of  $\text{HL}^1$  shows a strong band at  $1634 \text{ cm}^{-1}$ , and medium band at  $1277 \text{ cm}^{-1}$ , which are assigned to  $\nu(\text{C}=\text{N})$ <sup>[17]</sup> and phenolic  $\nu(\text{C}-\text{O})$  vibrations, respectively. In comparison with the IR

spectra of the Schiff bases, the first shifts by about  $18\text{--}36 \text{ cm}^{-1}$  of  $\nu(\text{C}=\text{N})$  and the second by about  $23\text{--}75 \text{ cm}^{-1}$  of  $\nu(\text{C}-\text{O})$  in the spectra of the complexes, which indicates the participation of imine nitrogen atoms and phenolic oxygen atoms in the coordination to the metal ion. This deduction agrees with the results of the X-ray crystal structure determinations.

The UV spectra of the ligands and the metal complexes were recorded in DMF solution at room temperature. In comparison with the absorption band of  $\text{HL}^1$  (325 nm), those of **1** and **2** are red-shifted by about  $16\text{--}18 \text{ nm}$ , which is evidence of  $\text{C}=\text{N}$  coordination to the metal center. Analogously, the UV band of  $\text{HL}^2$  (327 nm) is red-shifted by about  $2 \text{ nm}$  in

the spectrum of **3**. This phenomenon also shows that C=N is involved in coordination to the metal center.

### 3.2 | X-ray Structure Determination of Complexes

The structures of **1–3** were confirmed using X-ray diffraction. The crystal structures are discussed below.

#### 3.2.1 | Crystal structure of complex 1

Complex **1** crystallizes in the monoclinic space group  $C2/c$ , and its ORTEP structure (15% probability ellipsoids) along with the atomic numbering scheme is shown in Figure 1. The crystallographic data reveal that **1** has a distorted planar configuration and is four-coordinated by two phenolate oxygen atoms and two imine nitrogen atoms of two Schiff base ligands. Complex **1** has a crystallographic center that is right in the middle point of the Cu(II) ion in a seesaw conformation ( $\tau = 0.15$ ). The parameter  $\tau$  is defined as  $[360^\circ - (\alpha + \beta)]/141^\circ$  (where  $\beta = O(3)-Cu(1)-O(6)$ ,  $\alpha = N(6)-Cu(1)-N(3)$ ) and its value varies from 0 (in regular square planar geometry) to 1 (tetrahedral).<sup>[26]</sup> The ligands coordinate to the Cu(II) center in N–Cu–N and O–Cu–O *trans* geometries. The Cu–O (1.884(3) Å) and Cu–N (2.000(4) Å) bond distances and angles lie within the acceptable range and are comparable to those in other related systems.<sup>[27]</sup>

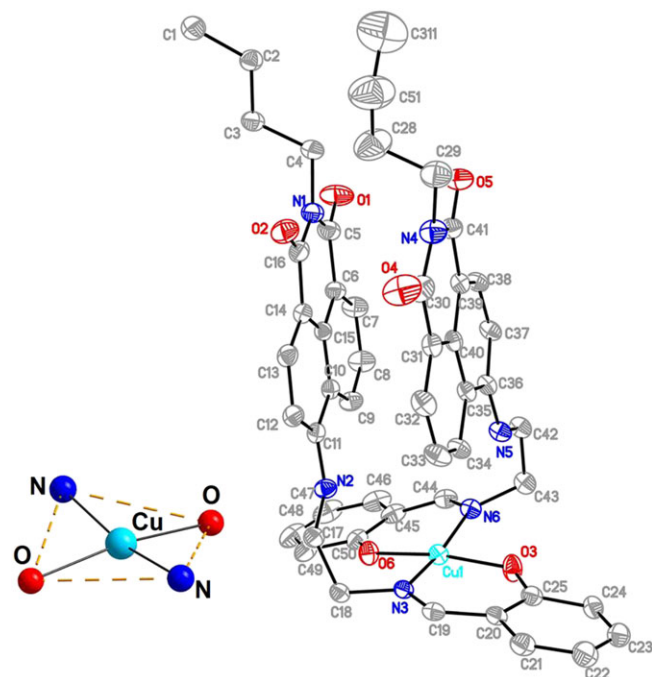


**FIGURE 1** Molecular structure and atom numberings of complex **1** showing displacement ellipsoids at the 15% probability level. Hydrogen atoms are omitted for clarity

The C=N bond distances are 1.292(6) Å and 1.303(5) Å (N(6)–C(44), C(19)–N(3)), which are consistent with a slight elongation of the C=N double bond when it coordinates to a metal center.<sup>[28]</sup> The O–Cu–N bond angles ( $O(3)-Cu(1)-N(6) = 87.81(15)^\circ$ ,  $O(6)-Cu(1)-N(6) = 92.42(15)^\circ$ ,  $O(3)-Cu(1)-N(3) = 92.13(14)^\circ$ ,  $O(6)-Cu(1)-N(3) = 89.61(15)^\circ$ ) are close to  $90^\circ$ . Moreover, the coordination of the two NO bidentate chelate ligands to the Cu(II) ion results in the formation of two six-membered rings (Cu(1)/O(6)/C(50)/C(45)/C(44)/N(6) and Cu(1)/O(3)/C(25)/C(20)/C(19)/N(3)). The crystal structure of **1** is stabilized by hydrogen bonds, and the neighboring chains are connected by C–H...O hydrogen bonds (Table 3), thus generating an infinite two-dimensional layer (Figure 2).

#### 3.2.2 | Crystal structure of complex 2

Complex **2** crystallizes in the triclinic space group P-1, and its ORTEP structure (15% probability ellipsoids) along with the atomic numbering scheme is shown in Figure 3. The crystallographic data reveal that **2** consists of two neutral  $[Zn(L)_2]$  and two pyridine molecules, and there are no coordinated water molecules. The crystal structure shows two crystallographically independent but chemically identical  $[Zn(L)_2(Py)]$ . Although Zn(1) and Zn(2) are five-coordinated with an  $N_3O_2$  ligand donor set and distorted square pyramidal geometry, their bond distances and angles are different. The bond distances between the zinc ion and the apical nitrogen atom, i.e. Zn(1)–N(6A) and Zn(2)–N(75), are 2.100(5) and 2.056(1) Å, respectively. The value of  $\tau$  is obtained from  $(\beta - \alpha)/60$  and it varies from 0 (in regular square pyramidal geometry) to 1 (trigonal bipyramidal).<sup>[29]</sup> According to the  $\tau$  value we find the geometry of Zn(1) ( $\tau = 0.151$ , where  $\beta = O(3)-Zn(2)-O(4)$ ,  $\alpha = N(7)-Zn(1)-N(0AA)$ ) is more distorted than Zn(2) ( $\tau = 0.145$ , where  $\beta = O(1)-Zn(1)-O(2)$ ,  $\alpha = N(6)-Zn(2)-N(3)$ ).

#### 3.2.3 | Crystal structure of complex 3

Complex **3** crystallizes in the monoclinic space group  $P2(1)/c$ , and its ORTEP structure (15% probability ellipsoids) along with the atomic numbering scheme is shown in Figure 4. The crystallographic data reveal that the molecular unit is

**TABLE 3** Intermolecular hydrogen bonds for complex **1**

D–H...A	D(D–H)	d(H...A)	d(D...A)	$\angle(DHA)$
C(2)–H(2A)...O(1)#4	0.97	2.51	3.175(7)	125.7
C(18)–H(18A)...O(5)#2	0.97	2.48	3.427(6)	163.8

Symmetry transformations used to generate equivalent atoms: #2  $x, -y + 1, z - 1/2$ ; #4  $-x, -y + 1, -z + 1$ .

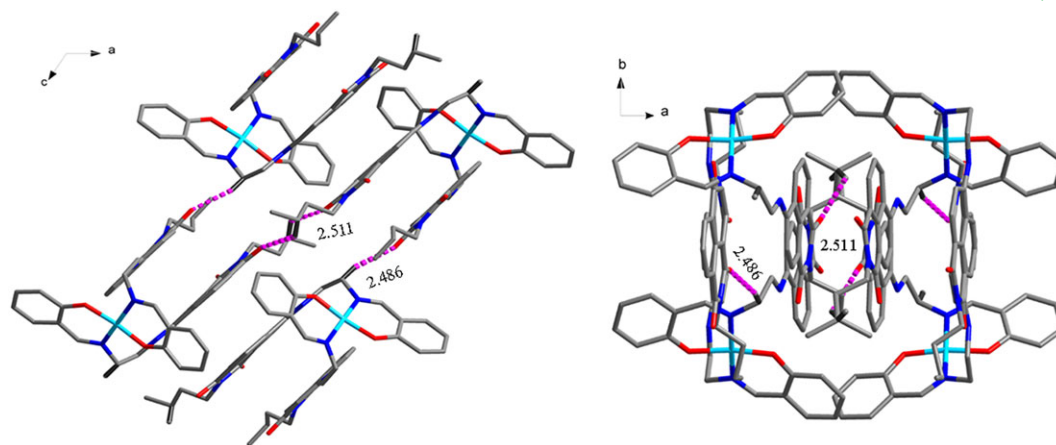


**FIGURE 2** Two-dimensional layer generated by C–H...O hydrogen bonding in the (a) *a*–*c* plane and (b) *a*–*b* plane in complex **1** (some atoms are omitted for clarity)

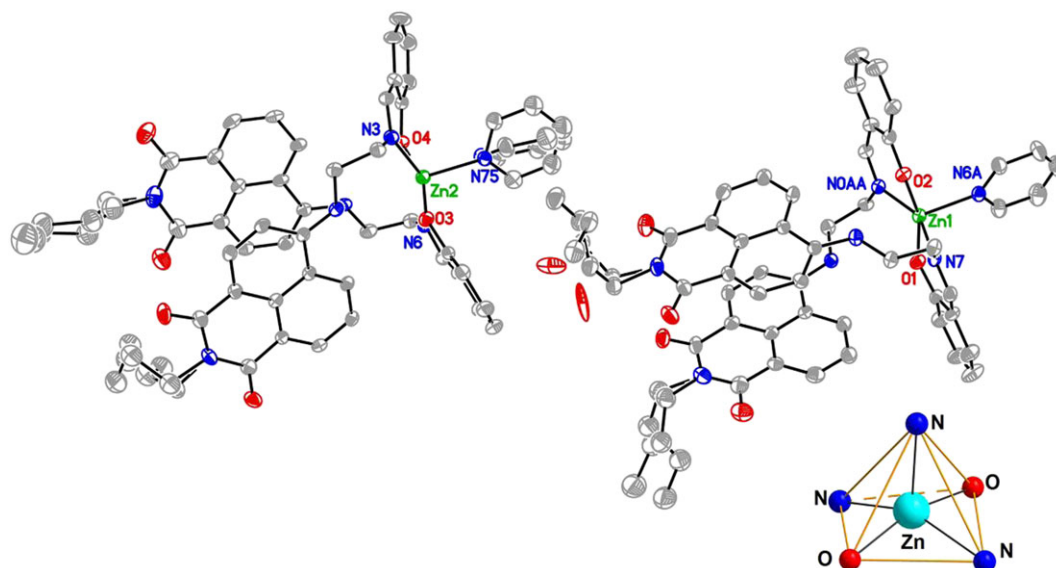


**FIGURE 3** Molecular structure and atom numberings of complex **2** showing displacement ellipsoids at the 15% probability level. Hydrogen atoms are omitted for clarity

centrosymmetric and is made up of equivalent halves. The symmetry transformations  $-x + 1$ ,  $-y + 1$ ,  $-z$  and  $x$ ,  $y$ ,  $z$  are used to generate equivalent atoms. All the equivalent bond lengths and angles around Ni(II) are equal (Table 2). Complex **3** comprises neutral  $[\text{Ni}(\text{L}^2)_2]$  and two DMF molecules. The ligands coordinate to the Ni(II) center in a *trans* geometry with respect to each other.  $[\text{Ni}(\text{L}^2)_2(\text{DMF})_2]$  has a crystallographic center of symmetry that is right in the middle point of the Ni(II) ion in a six-coordinate structure consisting of  $\text{N}_2\text{O}_4$  (two O5 atoms from two DMF molecules, two phenolate O1 atoms and two imine N1 atoms of two Schiff base ligands  $\text{HL}^2$ ) as shown in Figure 4. The coordination geometry of Ni(II) may be best described as slightly distorted octahedral with (N1,O1,N1A,O1A) providing the equatorial

plane. The maximum deviation distance (N1) from the least squares plane calculated from the four coordination atoms is 0 Å, and the nickel atom is also 0 Å. That means N1, O1, N1A, O1A and Ni(II) are coplanar as shown in Figure 4. The distances between the two axial atoms O5 and the equatorial plane are equivalent at 2.141(6) Å. However the angles of the two group atoms (O1–Ni1–O5) and (O1A–Ni1–O5) in axial positions are 89.48(9)° and 90.52(9)°, respectively. Therefore, compared with a regular octahedron, it reflects a relatively distorted coordination octahedron around the central Ni(II) atom.<sup>[30]</sup>

In addition, the structure shows the neighboring chains are connected by C–H...O hydrogen bonds (Table 4). Complex **3** forms an infinite two-dimensional layer through

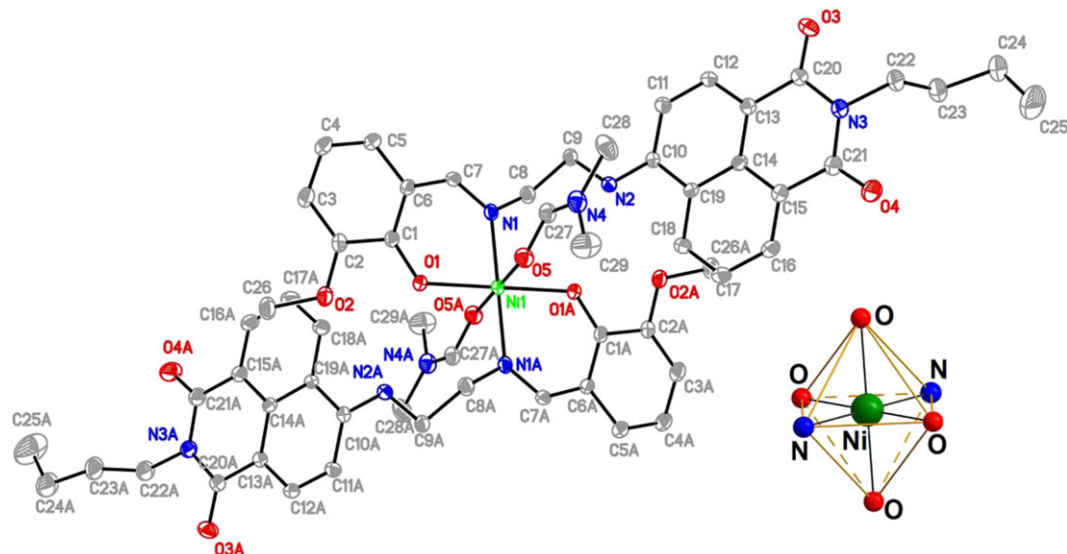


**FIGURE 4** Molecular structure and atom numberings of complex **3** showing displacement ellipsoids at the 15% probability level. Hydrogen atoms are omitted for clarity

intermolecular hydrogen bonds, which facilitate the stability of the bulk structure (Figure 5).

**TABLE 4** Intermolecular hydrogen bonds for complex **3**

D–H...A	<i>D</i> (D–H)	<i>d</i> (H...A)	<i>d</i> (D...A)	∠(DHA)
C(26)–H(26B)...O(4)#3	0.96	2.466	3.377(5)	158.2

Symmetry transformations used to generate equivalent atoms: #3  $-x + 1, y + \frac{1}{2}, -z + \frac{1}{2}$ .

### 3.3 | Thermal Analyses of Complexes 1–3

To study the stabilities of the three complexes, thermogravimetric analysis under nitrogen atmosphere was performed with a heating rate of  $10\text{ }^{\circ}\text{C min}^{-1}$ . As shown in Figure 6, complex **1** revealed only a one-step mass-loss process. The starting decomposition temperature of **1** was  $290\text{ }^{\circ}\text{C}$ . The successive mass loss at  $290\text{ }^{\circ}\text{C}$  to above  $800\text{ }^{\circ}\text{C}$  may be attributed to the gradual removal of ligand and the remainder of CuO. Complex **2** displayed a first weight loss region

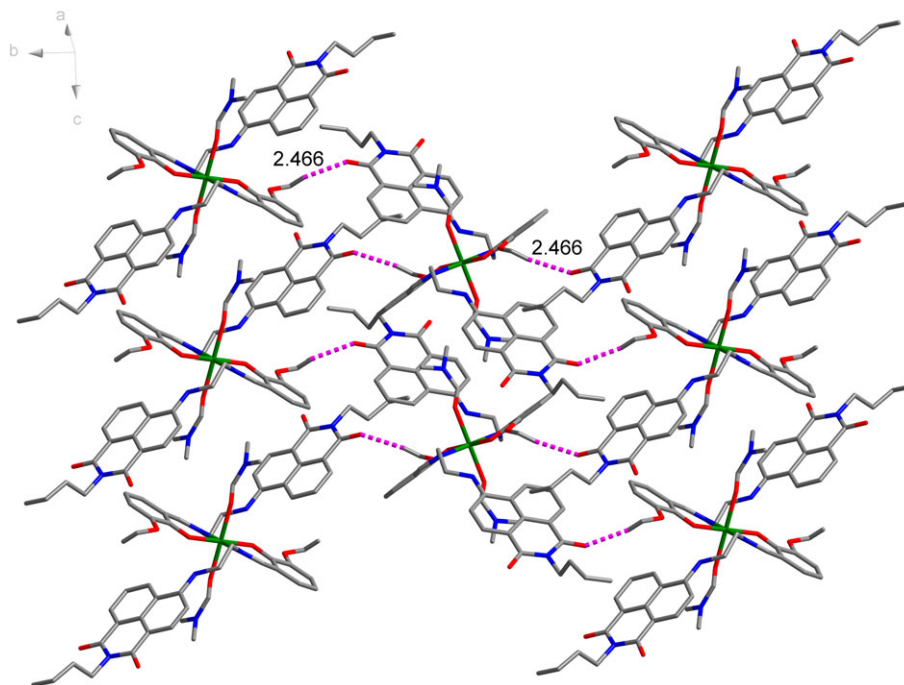


**FIGURE 5** Two-dimensional layer generated by C–H...O hydrogen bonding in complex **3** (some atoms are omitted for clarity)

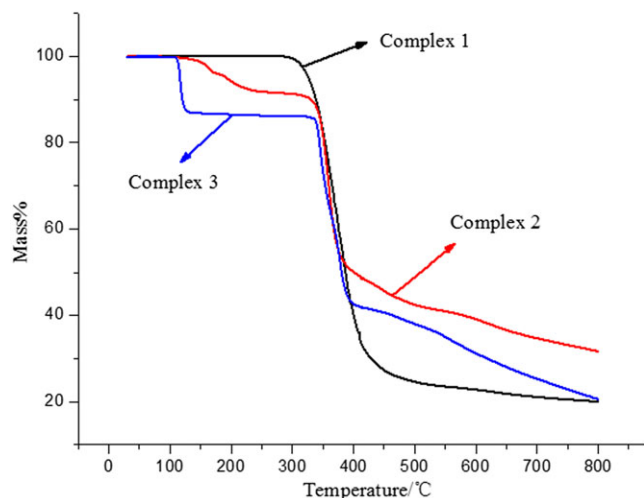


FIGURE 6 Thermogravimetric analysis curves of complexes 1–3

from 107 to 270 °C, assigned to release of the pyridine molecule and water of crystallization (found 9.0%, calcd 8.9%). Then, there was the appearance of a plateau region observed

from 270 to 323 °C. The subsequent mass loss at 323 °C to above 800 °C is explained on the basis of the stepwise removal of ligand and the remainder of ZnO. Complex 3 exhibited a process similar to that of 2, with the first weight loss region from 102 to 144 °C due to the loss of DMF molecules (found 13.1%, calcd 13.4%). Thereafter, there was the appearance of a flat region observed from 144 to 330 °C. The successive mass loss from 330 to above 800 °C may be the result of the gradual removal of ligand and the remainder of NiO.

### 3.4 | Photoluminescence Properties of Free Ligands and Complexes

The fluorescent emission spectra of the ligands (HL<sup>1</sup> and HL<sup>2</sup>) and their three complexes were measured in the solid state at room temperature as shown in Figure 7(a)–(c). Figure 7(d) depicts the color and luminescence changes for these compounds under ambient light and UV light (365 nm). The free ligands HL<sup>1</sup> and HL<sup>2</sup> show green luminescence with maximum wavelengths at 527 and 538 nm

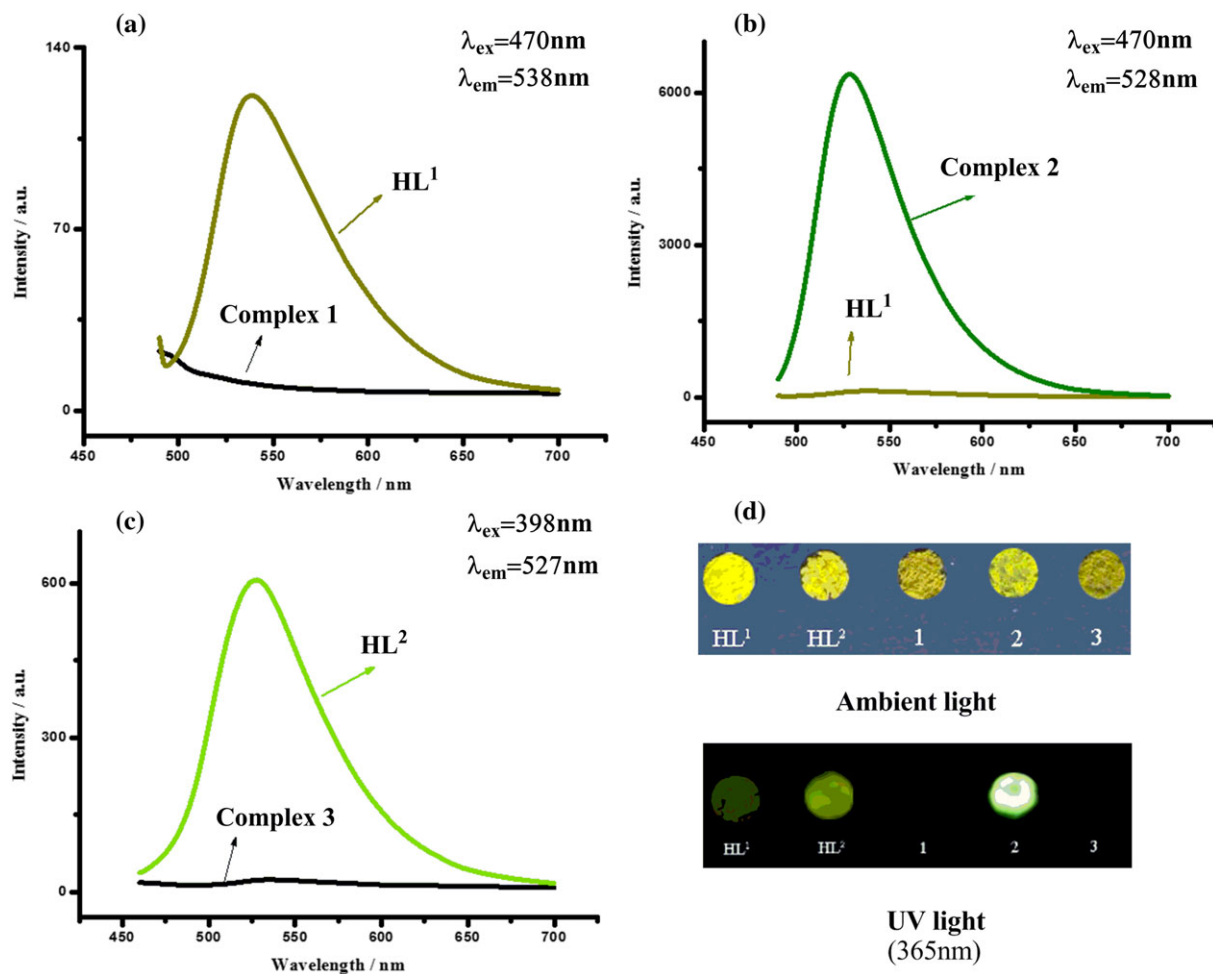


FIGURE 7 (a–c) Solid-state fluorescence emission spectra of ligands and complexes. (d) Photographic images of ligands and complexes under ambient light and UV light (365 nm)

when excited at 470 and 398 nm, respectively, significantly assigned to  $\pi$ - $\pi^*$  transition fluorescence. In comparison with HL<sup>1</sup>, complex **2** displays strong fluorescence due to the fact that the Zn(II) is difficult to oxidize or reduce owing to the stable  $d^{10}$  configurations.<sup>[31]</sup> On the other hand, the enhancement of the fluorescence intensity may be due to the coordination of free ligand to Zn(II), which reduces the dissipation of energy through radiationless thermal vibrations of the intra-ligand excited states and due to an enhancement of the rigidity of the ligand.<sup>[32]</sup> During complexation, quenching of fluorescence of complexes **1** and **3** is a somewhat common phenomenon, which is attributed to processes such as magnetic perturbation, redox activity, unpaired electrons, heavy-atom effects and electronic energy transfer.<sup>[32–34]</sup>

### 3.5 | Electrochemical Studies

The electrochemical properties of **1–3** were studied in DMF using cyclic voltammetry. Experimental results show that only **1** has a redox couple. The data are collected in Table 5 and a voltammogram is shown in Figure 8. The Cu(II) complex exhibits a pair of cathodic and anodic waves. The separation between the cathodic and anodic peak potentials  $\Delta E_p$  ( $E_{pa} - E_{pc}$ ) is greater than 60 mV, and the current  $i_{pa}/i_{pc} > 1$ , indicating an electrochemically irreversible process which can be assigned to the Cu(II)/Cu(I) couple.<sup>[35]</sup> The neutral uncomplexed Schiff base ligands are not electroactive over the range  $-1.5$  to  $+1.5$  V.

**TABLE 5** Electrochemical data for complex **1**<sup>a</sup>

$E_{pc}$	$E_{pa}$	$\Delta E_p$	$E_{1/2}$	$i_{pa}$	$i_{pc}$	$I$
-0.092	0.180	0.272	0.016	3.210	-2.633	1.219

$$^a \Delta E = E_{pa} - E_{pc}; E_{1/2} = (E_{pa} + E_{pc})/2; I = i_{pa}/i_{pc}.$$

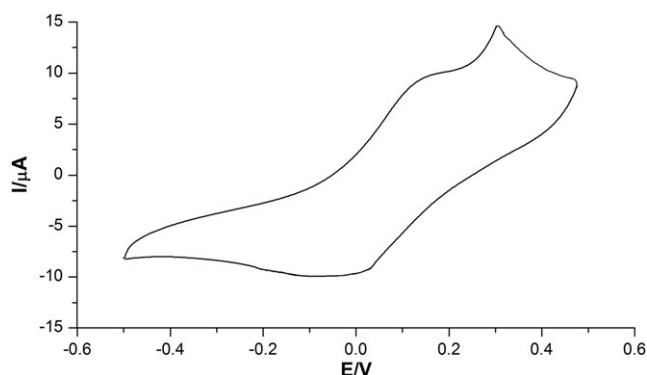


**FIGURE 8** Cyclic voltammogram of **1** recorded with a platinum electrode in DMF solution containing  $(nBu)_4N \cdot ClO_4$  (0.1 M) (scan rate =  $0.10 \text{ V s}^{-1}$ )

According to previous reports,<sup>[36]</sup> a transition metal complex must have a redox potential below 0.65 V ( $E^\circ(O_2-O_2^-)$ ) and above  $-0.33$  V ( $E^\circ(O_2-O_2^-)$ ) such that catalysis can be an effective mimic of SOD but toxic singlet oxygen cannot be formed; so the redox potential 0.272 V shows that **1** may have SOD activity.

### 3.6 | Antioxidant Activities

It has been reported that reactive oxygen species, such as hydroxyl radical ( $OH^\bullet$ ) and superoxide anion ( $O_2^{\bullet-}$ ), are involved in the pathogenesis of various diseases through direct effects on DNA and by acting as tumor promoters.<sup>[37,38]</sup> Therefore, the antioxidant activities of complexes **1–3** and their ligands were also studied. It was found that complex **2** did not possess antioxidant activity.

#### 3.6.1 | Hydroxyl radical scavenging activity

Some transition metal complexes can show antioxidant activity, as reported in the literature.<sup>[39–41]</sup> We compared the abilities of the metal complexes to scavenge hydroxyl radicals with those of the well-known natural antioxidants mannitol and vitamin C, using the same method as reported previously.<sup>[42,43]</sup> The 50% inhibitory concentration ( $IC_{50}$ ) values of mannitol and vitamin C are about  $9.6 \times 10^{-3}$  and  $8.7 \times 10^{-3}$  M, respectively. Figure 9(a)–(d) show plots of the hydroxyl radical scavenging effect for the complexes and their ligands; the  $IC_{50}$  values of complexes **1** and **3** are  $3.40 \times 10^{-5}$  and  $1.10 \times 10^{-5}$  M and those of HL<sup>1</sup> and HL<sup>2</sup> are  $9.62 \times 10^{-5}$  and  $1.25 \times 10^{-5}$  M, respectively, which imply that the ligands and **1** and **3** exhibit better scavenging activity than mannitol and vitamin C. It can be concluded that scavenging activity is exhibited by the free ligands and the synergistic effect of metal ions enhances the scavenging activity. The lower  $IC_{50}$  values observed in antioxidant assays demonstrate that **1**, **3** and Schiff base ligands have a strong potential to be applied as scavengers to eliminate radicals.

#### 3.6.2 | Superoxide radical scavenging activity

As another significant assay of antioxidant activity, superoxide radical ( $O_2^{\bullet-}$ ) scavenging activity of the complexes and ligands was investigated. HL<sup>1</sup>, HL<sup>2</sup>, **1** and **3** show  $IC_{50}$  values of  $1.69 \times 10^{-5}$ ,  $2.33 \times 10^{-5}$ ,  $1.60 \times 10^{-6}$  and  $2.70 \times 10^{-5}$  M, respectively, as shown in Figure 9(e)–(h). Complex **1** has better superoxide radical scavenging activity than the ligands and **3**. The reason for this phenomenon may be due to the relatively high activity, which is derived from the change of valence of Cu(II) ions. The results show that **1** also exhibits

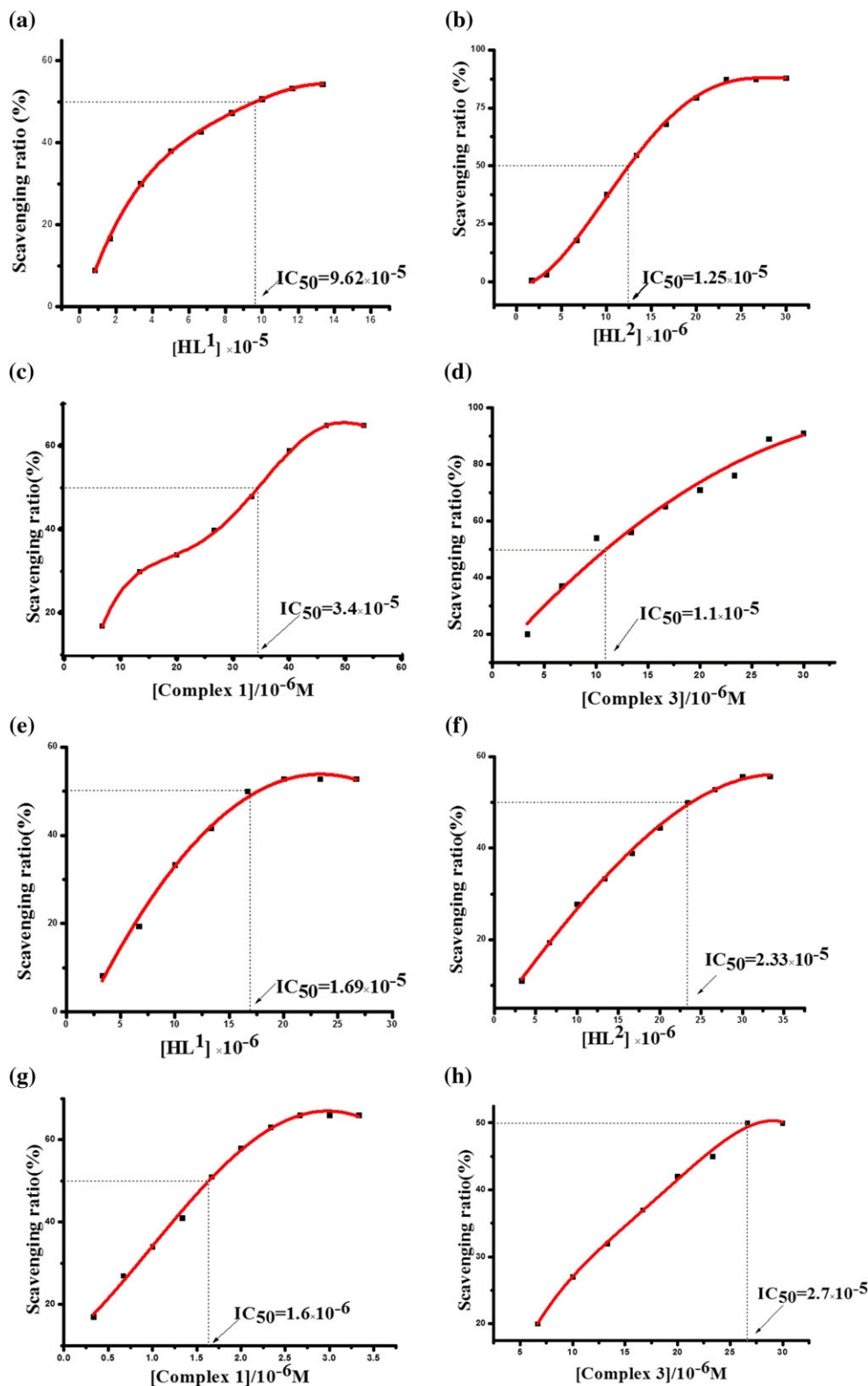


**FIGURE 9** Plots of antioxidant properties for ligands and complexes. Hydroxyl radical scavenging effect of (a)  $HL^1$ , (b)  $HL^2$ , (c) **1** and (d) **3**. Superoxide radical scavenging effect of (e)  $HL^1$ , (f)  $HL^2$ , (g) **1** and (h) **3**

good SOD activity relative to the standard SOD complex ( $IC_{50} = 2.6 \times 10^{-5}$  M).<sup>[44]</sup> We find that **1** has excellent suppression ratio for  $O_2^{\cdot-}$ , consistent with the electrochemical studies.

The lower  $IC_{50}$  values observed in hydroxyl radical and superoxide radical scavenging assays demonstrate that complexes **1** and **3** and their ligands have some scavenging effects for  $HO^{\cdot}$  and  $O_2^{\cdot-}$ .

## 4 | CONCLUSIONS

Schiff base ligands and their complexes have been synthesized and characterized. Single-crystal X-ray diffraction analysis shows complexes **1–3** have four-, five- and six-coordinated geometries, respectively. Experimental results indicate that **2** shows stronger luminescence than the other compounds in the solid state. Electrochemical studies show irreversible redox behavior for **1**. Moreover, **1** and **3** exhibit potential antioxidant activities against HO<sup>•</sup> and O<sub>2</sub><sup>•-</sup> radicals from *in vitro* studies. These findings indicate that the transition metal complexes have many potential practical applications for the development of luminescence, electrochemistry and new therapeutic reagents for diseases at the molecular level.

## ACKNOWLEDGMENTS

The present research was supported by the National Natural Science Foundation of China (grant no. 21367017), Natural Science Foundation of Gansu Province (grant no. 1212RJZA037) and Graduate Student Innovation Projects of Lanzhou Jiaotong University.

## REFERENCES

- [1] M. R. Maurya, A. Kumar, A. R. Bhat, A. Azam, C. Bader, D. Rehder, *Inorg. Chem.* **2006**, *45*, 1260.
- [2] a) S. Ray, S. Konar, A. Jana, K. Das, A. Dhara, S. Chatterjee, S. K. Kar, *J. Mol. Struct.* **2014**, *1058*, 213; b) S. Ray, S. Konar, A. Jana, K. Das, R. J. Butcher, T. K. Mondal, S. K. Kar, *Polyhedron* **2013**, *50*, 51; c) S. Koner, S. Saha, T. Mallah, K. I. Okamoto, *Inorg. Chem.* **2004**, *43*, 840; d) A. K. Sah, T. Tanase, M. Mikuriya, *Inorg. Chem.* **2006**, *45*, 2083.
- [3] Q. F. Han, F. F. Jian, L. D. Lu, X. J. Yang, X. J. Wang, *Chem. Crystallogr.* **2001**, *31*, 247.
- [4] A. Erxleben, D. Schumacher, *Eur. J. Inorg. Chem.* **2001**, *2001*, 3039.
- [5] a) M. R. Bermejo, A. M. Gonzalez-Noya, V. Abad, M. I. Fernandez, M. Maneiro, R. Pedrido, M. Vazquez, *Eur. J. Inorg. Chem.* **2004**, *2004*, 3696; b) Y. B. Jiang, H. Z. Kou, R. J. Wang, A. L. Cui, *Eur. J. Inorg. Chem.* **2004**, *2004*, 4608; c) W. K. Dong, J. T. Zhang, Y. J. Dong, Y. Zhang, Z. K. Wang, *Z. Anorg. Allg. Chem.* **2016**, *642*, 189; d) W. K. Dong, F. Zhang, N. Li, L. Xu, Y. Zhang, J. Zhang, L. C. Zhu, *Z. Anorg. Allg. Chem.* **2016**, *642*, 532; e) W. K. Dong, Y. X. Sun, G. H. Liu, L. Li, X. Y. Dong, X. H. Gao, *Z. Anorg. Allg. Chem.* **2012**, *638*, 1370.
- [6] H. C. Lin, *Synth. React. Inorg. Met.-Org. Chem.* **1993**, *23*, 1097.
- [7] R. K. Agarwal, P. Garg, H. Agarwal, D. Chandra, *Synth. React. Inorg. Met.-Org. Chem. Nano-Met. Chem.* **1997**, *27*, 251.
- [8] L. Singh, N. Tyagi, N. P. Dhaka, S. K. Sindhu, *Asian J. Chem.* **1999**, *11*, 503.
- [9] a) S. Y. Yu, S. X. Wang, Q. H. Luo, L. F. Wang, *Polyhedron* **1993**, *12*, 1097; b) M. J. Clare, J. D. Heeschele, *Bioinorg. Chem.* **1973**, *2*, 187; c) A. A. Jarrahpour, M. Motamedifar, K. Pakshir, N. Hadi, M. Zarei, *Molecules* **2004**, *9*, 815; d) M. Proetto, W. Liu, A. Hagenbach, U. Abram, R. Gus, *Eur. J. Med. Chem.* **2012**, *53*, 168; e) S. Sobha, R. Mahalakshmi, N. Raman, *Spectrochim. Acta A* **2012**, *92*, 175. f) S. Rekha, K. R. Nagasundara, *Indian J. Chem.* **2006**, *45*, 2421.
- [10] P. Hrdlovič, Š. Chmela, M. Danko, M. Sarakha, G. Guyot, *J. Fluoresc.* **2008**, *18*, 393.
- [11] Z. F. Tao, X. Qian, *Dyes Pigments* **1999**, *43*, 139.
- [12] E. Martin, R. Weigand, A. Pardo, *J. Lumin.* **1996**, *68*, 157.
- [13] a) H. Tian, J. Gan, K. Chen, J. He, Q. Song, X. Hou, *J. Mater. Chem.* **2002**, *12*, 1262; b) I. Grabchev, J. M. Chovelon, X. Qian, *J. Photochem. Photobiol. A* **2003**, *158*, 37; c) J. Morgado, J. Gruner, S. P. Walcott, T. M. Yong, R. Cervini, S. C. Moratti, A. B. Holmes, R. H. Friend, *Synth. Met.* **1998**, *95*, 113.
- [14] E. Tamanini, A. Katewa, L. Sedger, M. Todd, M. Watkinson, *Inorg. Chem.* **2009**, *48*, 319.
- [15] S. Chatterjee, S. Pramanik, S. U. Hossain, S. Bhattacharya, S. C. Bhattacharya, *J. Photochem. Photobiol. A* **2007**, *187*, 64.
- [16] T. Martynski, K. Mykowska, D. Bauman, *J. Mol. Struct.* **1994**, *325*, 161.
- [17] a) H. L. Wu, G. L. Pan, Y. C. Bai, Y. H. Zhang, H. Wang, F. R. Shi, X. L. Wang, J. Kong, *J. Photochem. Photobiol. B* **2014**, *135*, 33; b) H. L. Wu, Y. C. Bai, Y. H. Zhang, *J. Coord. Chem.* **2014**, *67*, 3054; c) H. L. Wu, F. Jia, F. Kou, B. Liu, J. K. Yuan, Y. Bai, *Transit. Met. Chem.* **2011**, *36*, 847.
- [18] B. Liu, H. Tian, *Chem. Commun.* **2005**, *25*, 3156.
- [19] Bruker, *SMART, SAINT and SADABS*, Bruker AXS Inc., Madison, WI **2000**.
- [20] G. M. Sheldrick, *SHELXTL*, Siemens Analytical X-Ray Instruments Inc., Madison, WI **1996**.
- [21] M. Xu, Y. C. Zhang, Z. H. Xu, Z. Z. Zeng, *Inorg. Chim. Acta* **2012**, *384*, 324.
- [22] C. C. Winterbourn, *Biochem. J.* **1981**, *198*, 125.
- [23] Z. Y. Guo, R. E. Xing, S. Liu, H. H. Yu, P. B. Wang, C. P. Li, P. C. Li, *Bioorg. Med. Chem. Lett.* **2005**, *15*, 4600.
- [24] X. Y. Le, S. R. Liao, X. P. Liu, X. L. Feng, *J. Coord. Chem.* **2006**, *59*, 985.
- [25] Q. H. Luo, Q. Lu, A. B. Dai, L. G. Huang, *J. Inorg. Biochem.* **1993**, *51*, 655.
- [26] L. Yang, D. R. Powell, R. P. Houser, *Dalton Trans.* **2007**, *9*, 955.
- [27] a) W. K. Dong, J. Zhang, Y. Zhang, N. Li, *Inorg. Chim. Acta* **2016**, *444*, 95; b) H. L. Wu, F. Jia, F. Kou, B. Liu, J. K. Yuan, Y. Bai, *J. Coord. Chem.* **2011**, *64*, 3454; c) H. L. Wu, F. Kou, F. Jia, B. Liu, J. K. Yuan, Y. Bai, *J. Photochem. Photobiol. B* **2011**, *105*, 190; d) W. K. Dong, Y. X. Sun, S. J. Xing, Y. Wang, X. H. Gao, *Z. Naturforsch. B* **2012**, *67b*, 197; e) W. K. Dong, G. Wang, S. S. Gong, J. F. Tong, Y. X. Sun, X. H. Gao, *Transit. Met. Chem.* **2012**, *37*, 271; f) H. Karabiyik, O. Erdem, M. J. Aygun, *Inorg. Organometal. Polym.* **2010**, *20*, 142; g) P. Mukherjee, M. G. B. Drew, A. Figuerola, *Polyhedron* **2008**, *27*, 3343; h) L. Mouni, M. Akkurt, S. O. Yildirm, *J. Chem. Crystallogr.* **2010**, *40*, 169.
- [28] a) J. C. Ma, X. Y. Dong, W. K. Dong, Y. Zhang, L. C. Zhu, J. T. Zhang, *J. Coord. Chem.* **2016**, *69*, 149; b) W. K. Dong, G. H. Liu, Y. X. Sun, X. Y. Dong, X. H. Gao, *Z. Naturforsch. B* **2012**,

- 67b, 17; c) I. Aiello, A. Crispini, M. Ghedini, M. La Deda, F. Barigelletti, *Inorg. Chim. Acta* **2000**, *308*, 121.
- [29] S. Youngme, J. Phatchimkun, U. Sukangpanya, C. Pakawatchai, N. Chaichit, P. Kongsaree, J. Krzystek, B. Murphy, *Polyhedron* **2007**, *26*, 871.
- [30] a) W. K. Dong, L. C. Zhu, J. C. Ma, Y. X. Sun, Y. Zhang, *Inorg. Chim. Acta* **2016**, *453*, 402; b) W. K. Dong, Y. X. Sun, L. Li, S. T. Zhang, L. Wang, X. Y. Dong, X. H. Gao, *J. Coord. Chem.* **2012**, *65*, 2332; c) H. L. Wu, X. C. Huang, J. K. Yuan, F. Kou, G. S. Chen, B. B. Jia, Y. Yang, Y. L. Lai, *Z. Naturforsch. B* **2010**, *65b*, 1334; d) L. E. Xiao, M. Zhang, W. H. Sun, *Polyhedron* **2010**, *29*, 142; e) D. Kang, J. Seo, S. Y. Lee, J. Y. Lee, *Inorg. Chem. Commun.* **2007**, *10*, 1425; f) N. Yoshikawa, S. Yamabe, N. Kanehisa, Y. Kai, H. Takashima, K. Tsukahara, *Eur. J. Inorg. Chem.* **2007**, *13*, 1911; g) J. P. Collin, I. M. Dixon, J. P. Sauvage, J. A. G. Williams, F. Barigelletti, L. Flamigni, *J. Am. Chem. Soc.* **1999**, *121*, 5009.
- [31] S. Basak, S. Sen, S. Banerjee, S. Mitra, G. Rosair, M. T. G. Rodriguez, *Polyhedron* **2007**, *26*, 5104.
- [32] Q. Ye, X. B. Chen, Y. M. Song, X. S. Wang, J. Zhang, R. G. Xiong, H. K. Fun, X. Z. You, *Inorg. Chim. Acta* **2005**, *358*, 1258.
- [33] G. B. Bagihalli, P. G. Avaji, S. A. Patil, P. S. Badami, *Eur. J. Med. Chem.* **2008**, *43*, 2639.
- [34] J. Chan, S. C. Dodani, C. J. Chang, *Nat. Chem.* **2012**, *4*, 973.
- [35] A. W. Addison, H. M. J. Hendriks, J. Reedije, L. K. Thompson, *Inorg. Chem.* **1981**, *20*, 103.
- [36] H. L. Wu, R. R. Yun, K. T. Wang, K. Li, X. C. Huang, T. Sun, Y. Y. Wang, *Z. Anorg. Allg. Chem.* **2010**, *636*, 1397.
- [37] R. M. Touyz, *Hypertension* **2004**, *44*, 248.
- [38] T. Fujimori, S. Yamada, H. Yasui, H. Sakurai, Y. In, T. Ishida, *J. Biol. Inorg. Chem.* **2006**, *10*, 831.
- [39] S. B. Bukhari, S. Memon, M. Mahroof-Tahir, M. I. Bhangar, *Spectrochim. Acta A* **2009**, *71*, 1901.
- [40] F. V. Botelho, J. I. Alvarez-Leite, V. S. Lemos, A. M. C. Pimenta, H. D. R. Calado, T. Matencio, C. T. Miranda, E. C. Pereira-Maia, *J. Inorg. Biochem.* **2007**, *101*, 935.
- [41] Q. Wang, Z. Y. Yang, G. F. Qi, D. D. Qin, *Eur. J. Med. Chem.* **2009**, *44*, 2425.
- [42] a) H. L. Wu, Y. H. Zhang, C. Y. Chen, J. W. Zhang, Y. C. Bai, F. R. Shi, X. L. Wang, *New J. Chem.* **2014**, *38*, 3688; b) H. L. Wu, F. R. Shi, X. L. Wang, Y. H. Zhang, Y. C. Bai, J. Kong, C. P. Wang, *Transit. Met. Chem.* **2014**, *39*, 261; c) H. L. Wu, J. K. Yuan, Y. Bai, G. L. Pan, H. Wang, J. Kong, X. Y. Fan, H. M. Liu, *Dalton Trans.* **2012**, *41*, 8829.
- [43] S. Satyanarayana, J. C. Daborusak, J. B. Chaires, *Biochemistry* **1993**, *32*, 2573.
- [44] R. N. Patel, D. K. Patel, V. P. Sondhiya, K. K. Shukla, Y. Singh, A. Kumar, *Inorg. Chim. Acta* **2013**, *405*, 209.

## SUPPORTING INFORMATION

Additional Supporting Information may be found online in the supporting information tab for this article.

**How to cite this article:** Xu Y, Zhang H, Shen K, Mao S, Shi X, Wu H. Four-, five- and six-coordinated transition metal complexes based on naphthalimide Schiff base ligands: Synthesis, crystal structure and properties. *Appl Organometal Chem.* 2017;e3902. <https://doi.org/10.1002/aoc.3902>